Open-source Numerical Modeling of Solidification Cracking Susceptibility: Application to Refractory Alloy Systems

Jeffrey W. Sowards, Fredrick N. Michael, Omar Mireles

Marshall Space Flight Center

Outline

- Problem & Motivation
- Background on the Model and Algorithm
- Algorithm Verification vs Past Aluminum Alloy Studies
- Algorithm Verification vs Past Refractory Alloys Weldability Data
- Extrapolations to Refractory-Interstitial (O,C,N) Binary Alloys
- Extending the Approach for Development of Hot Cracking Susceptibility Equations

Background on Refractory Metals

- Refractory metals and alloys are used for service in extreme high temperature environments:
  - Reaction Control System (RCS) thrusters
  - Space Nuclear Propulsion (SNP) clad and structure
  - Hypergolic / green propulsion chambers and catalyst
  - Electric propulsion grids
  - Power conversion system heat pipes and regenerators
  - Hypersonic wing leading edges

- Refractory metals are desirable due to:
  - High melt temperature (T_m)
  - Retain strength and hardness at elevated temperature
  - Corrosion and wear resistant (outside of propulsion)

- Aerospace refractory metal parts tend to be:
  - Thin-walled geometries (converging-diverging nozzles)
  - Relatively simple geometries
  - High buy-to-fly ratio (20:1 to 50:1)
  - Low production rate

Apollo CSM RCS using C103. Courtesy Aerojet-Rocketdyne

TZM alloy heat pipe. Courtesy Advanced Cooling Technologies.

Base	Name	Composition (wt%)
Nb	Nb	Nb
	Nb-1Zr	Nb-1Zr
	C103	Nb-10Hf-1Ti
	C129Y	Nb-10Hf-10W-0.1Y
	Cb752	Nb-10W-2.5Zr
	C3009	Nb-30Hf-10W
	WC3015	Nb-28Hf-13W-5Ti-2Ta-1Zr
	FS85	Nb-28Ta-10W-1Zr
Mo	Mo	Mo
	Mo-21Re	Mo-21Re
	Mo-41Re	Mo-41Re
	Mo-44Re	Mo-44Re
	Mo-47.5Re	Mo-47.5Re
	TZM	Mo-0.5Ti-0.08-Zr-0.2C
W	W	W
	W-25Re	W-25Re
Ta	Ta	Ta
	Ta-10W	Ta-10W
Ir	Ir	
	DOP26	Ir-0.3W-0.006Th-0.005Al
Re	Re	Re

Traditional Refractory Alloys

Green propulsion Re thruster.

X-51A hypersonic test vehicle. Courtesy USAF.

Problem and Goal: Fabricating Refractory Alloys

- Typically exhibit poor weldability. Existing alloys were design 60+ years ago and never optimized to be weldable and printable.
  - Thermal shock (thermal stress builds due to extreme high melting point)
  - Brittleness at room temperature (due to shift of ductile to brittle transition)
  - Solidification cracking (due to segregation of alloying elements and wide solidification temperature ranges induced by alloying)

- Traditional refractory manufacture is difficult and expensive:
  - Bar, plate, tube, sheet stocks and sizes limited (constrains design)
  - Powder feedstock are angular and not usually alloyed
  - High feedstock cost
  - Relatively difficult to form/machine (fracture prone)
  - Heat treatment requires specialized facilities (O, C, N sensitive)
  - Joining options limited (Usually electron beam welded)
  - Inspection options limited

- Alloys designed for traditional manufacture:
  - Powder metallurgy (CIP, HIP, deposition)
  - Forging
  - Wire and/or plunge EDM
  - W ($100/kg) or Mo ($80/kg) alloyed with 25-47.5 wt% Re ($2.76k/kg) to improve ductility

- **Goal. Develop new refractory alloys using a CALPHAD approach, optimized for printability with L-PBF L-DED and weldability by reducing solidification cracking susceptibility**

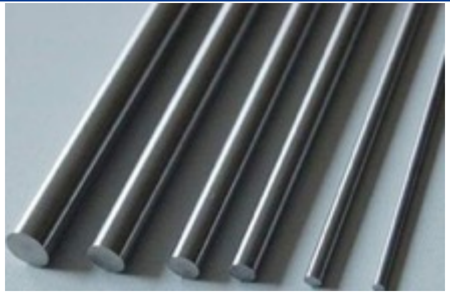

C103 forged bar stock.
Courtesy ATI.

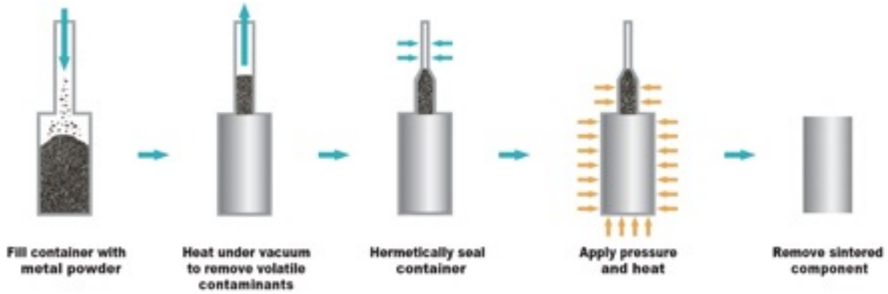

Hot Isostatic Press (HIP) process [1].

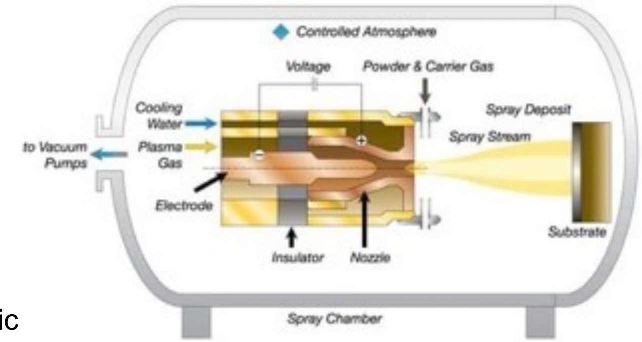

Vacuum Plasma Spray (VPS) process [2].

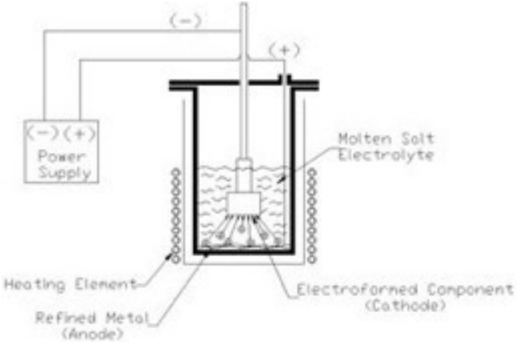

Electro Deposition / Forming process [3].

[1] https://www.malvernpanalytical.com/en/industries/advanced-manufacturing/powder-metallurgy/isostatic
[2] https://www.neodynamiki.gr/
[3] https://plasmapros.com/processes/

Model: Kou's Solidification Cracking Criterion

Kou's Cracking Criterion [4]: $\left\{ \underbrace{V_{local}}_{\text{(separation)}} > \underbrace{\phi\sqrt{1-\beta}\frac{d\sqrt{f_s}}{dT}\frac{dT}{dt}}_{\text{(growth)}} + \underbrace{\phi\frac{d}{dz}\left[\left(1-\sqrt{1-\beta}\sqrt{f_s}\right)v_z\right]}_{\text{(feeding)}} \right\}_{\sqrt{f_s}\to 1}$

- Considers a balance between grain boundary separation (cracking), lateral growth of grains, and liquid feeding between dendrites
  - v is velocity, ϕ is dendrite diameter, β is shrinkage, T is temperature, f_s is fraction solid
- Crack susceptibility increases as $|dT/d(f_S^{1/2})|$ increases near $f_S^{1/2} = 1$.
  - $f_S^{1/2}$ significance is similarity to dimensionless radius of dendrite
  - Steepness of solidification path near terminal solidification results in higher index: suggesting increased crack susceptibility due to slower transverse growth rate and longer passageway for feeding
- Criterion does not predict occurrence but rather susceptibility.
- The Scheil equation is used to predict the solidification path of an alloy, i.e., the plot of f_s vs T and usefully couples to this criterion for evaluating influence of composition.

Geometrical Significance

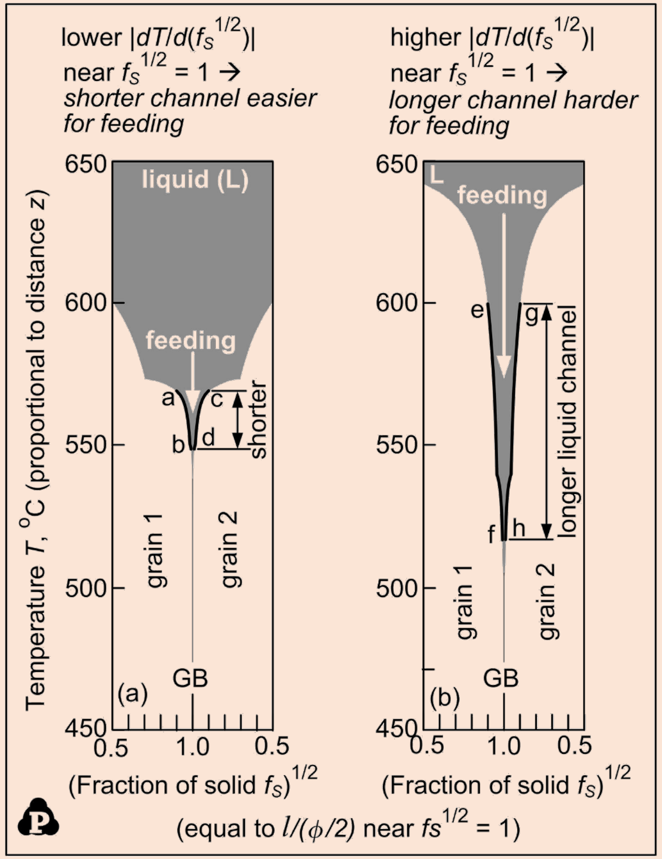

Composition Influence

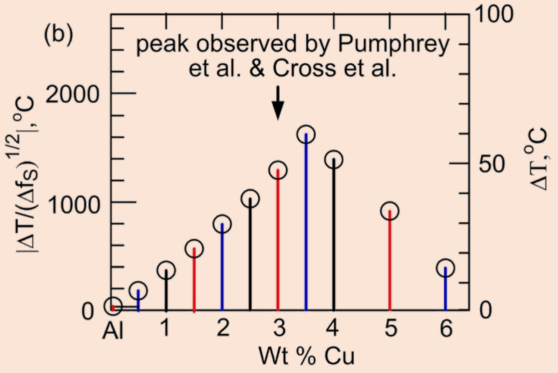

[4] Kou. Acta Mat 88 (2015): 366-374
https://doi.org/10.1016/j.actamat.2015.01.034

Process Flow and Algorithm to Compute Crack Susceptibility

In this work, we numerically implement calculation of Kou's CSI in a Jupyter Notebook with python scripting.

[5] de Walle et al. *Calphad* 61 (2018): 173-178 https://avdwgroup.engin.brown.edu/

[6] Otis & Liu. *J. Open Res. Soft.* 5 (2017): 1 https://pycalphad.org/

[7] Bocklund, et al. (2020). https://github.com/pycalphad/scheil

[4] Kou. *Acta Mat* 88 (2015): 366-374 https://doi.org/10.1016/j.actamat.2015.01.034

Database (.tdb) → pycalphad Equilibrium (or Thermocalc) → Scheil Solidification → Kou's Crack Susceptibility Index (CSI)

Jupyter Notebook Flow for pycalphad (Python 3)

```
import Dependencies #pycalphad and math packages
Variables = database, elements, phases
Conditions = start_temp, temp_step, filter #Scheil setup
Scheil = T vs fs plot #Calculate
fsnew = sqrt(fs) #take
PowerSmooth = savgol.(T,fsnew) #Savitsky-Golay power smoothing
derivative = abs(gradient(power_smooth) / gradient(fsnew))
Max_value = max(derivative) #between 0.9 and 0.99 fsnew

#Iterate for multiple elements to generate e.g., ternary:
for i in x_element
    for j in y_element
        Perform above

#Log data
#Perform postprocessing and plotting
```

Complete code examples are available in a report online. Plans to post on GitHub.
[8] Michael & Sowards (2023) NASA-TM-20230002218.
https://ntrs.nasa.gov/citations/20230002218

Example: Jupyter Notebook Output and CSI Calculation

1. Compute Scheil Solidification Path

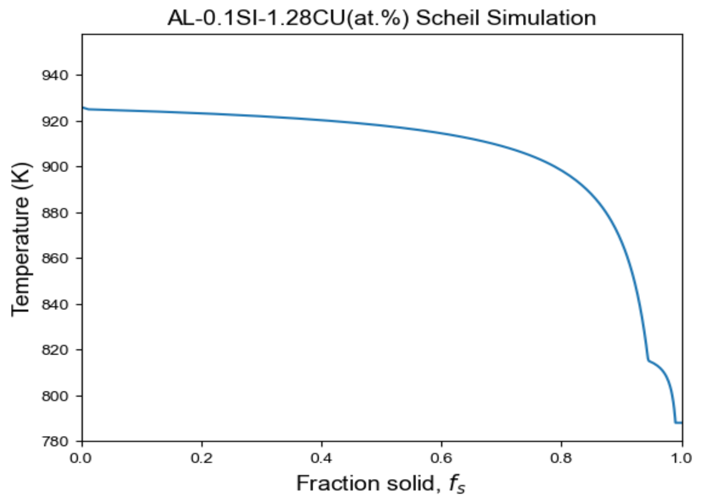

2. Perform Best Fit to fs$^{1/2}$-T Plot (optional)

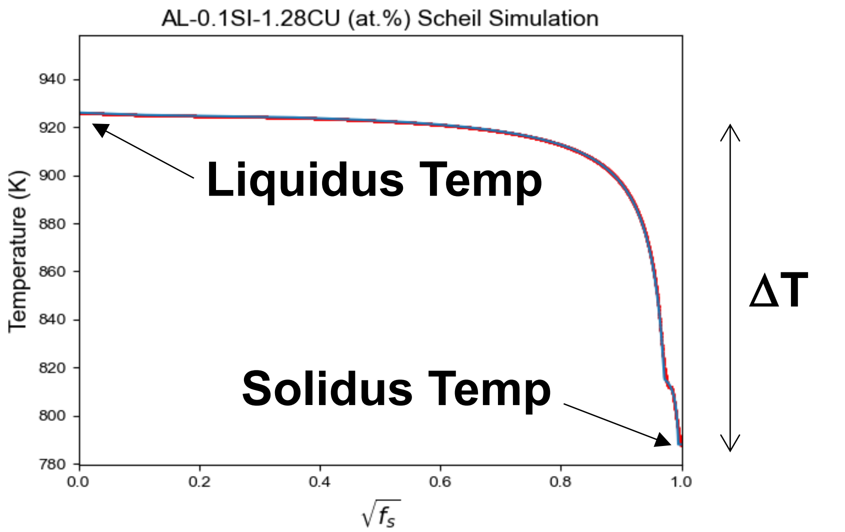

3. Compute Derivative of fs$^{1/2}$-T Best Fit Line

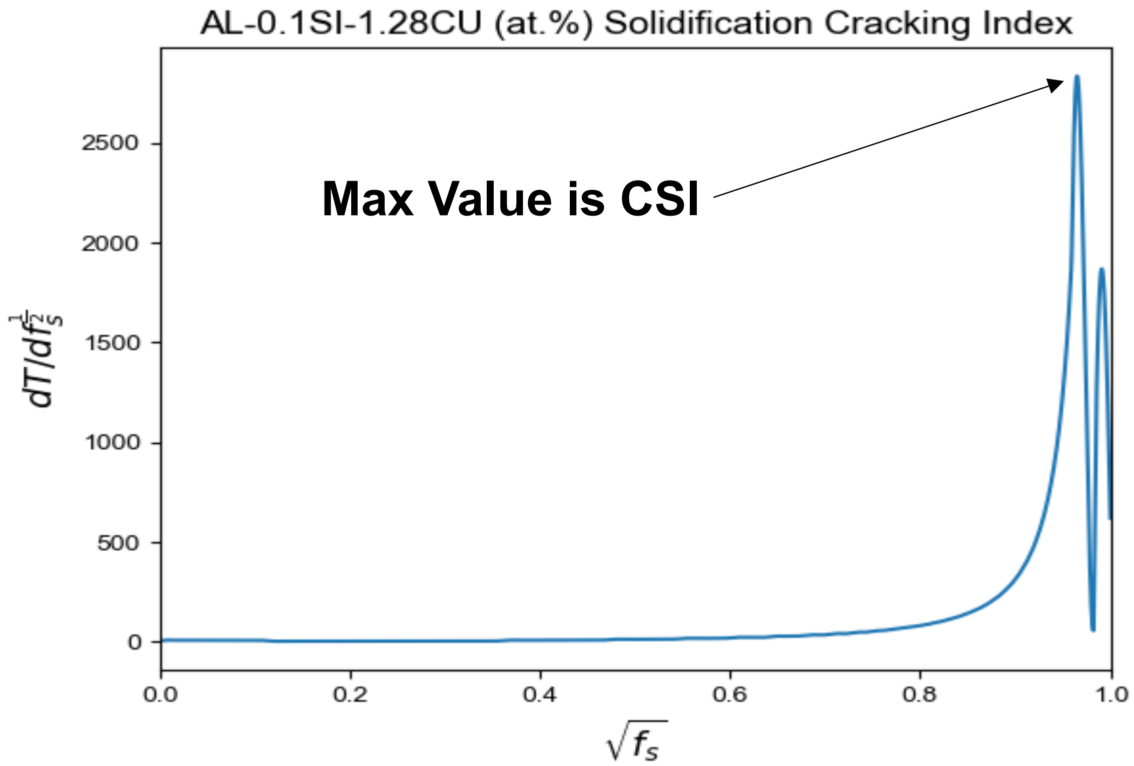

4. Find Max CSI and Log Results

Jupyter Notebook Output

```
Run # = 18 Total Run time = 166.1 seconds
Composition = {W_SI: 0.001, W_CU: 0.029724137931034483}
Max CSI = 2832.9 K, Max CSI with Filter = 2832.9 K, Solidus Temperature = 788.0 K
```

Algorithm Verification in Al-Si-Cu Ternary with Open-source Software

Liu and Kou's Cracking Index Map [9] produced with Pandat + Pan aluminum database. Solidification with no diffusion (Scheil).

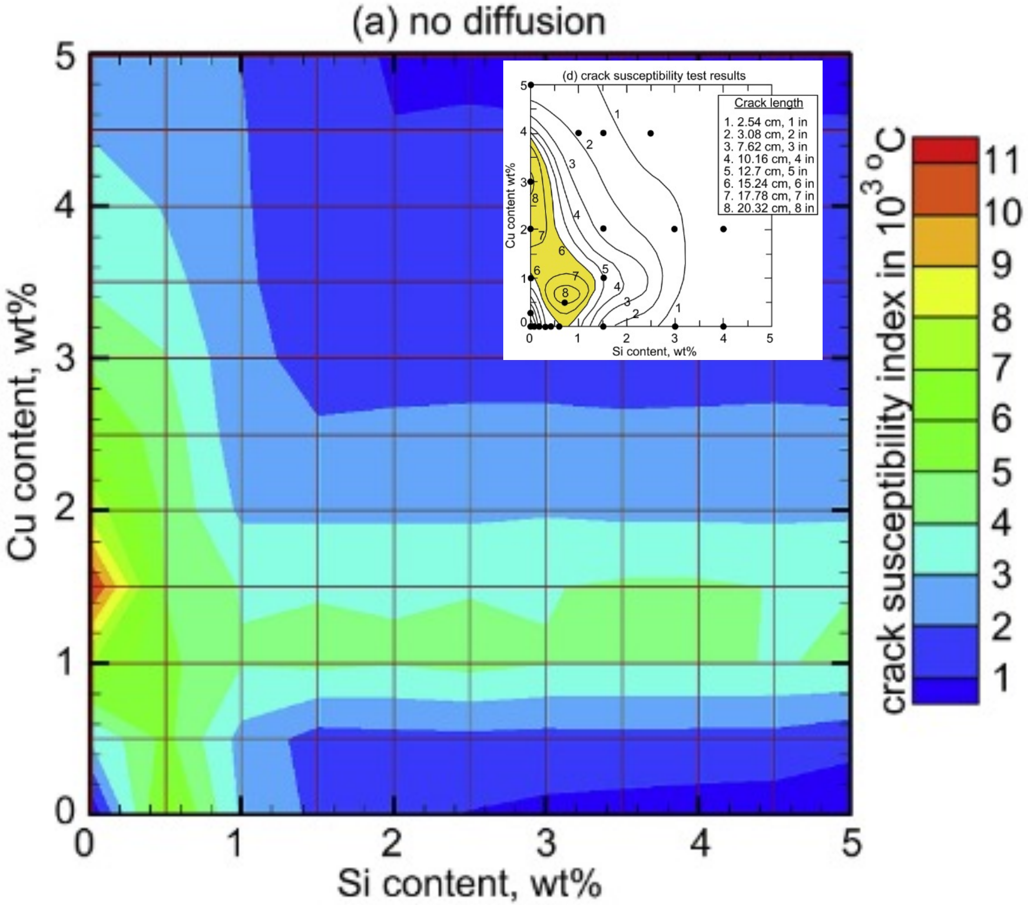

[9] Liu and Kou. *Acta Mat.* 125, 15 (2017): 513-523.
https://doi.org/10.1016/j.actamat.2016.12.028

Kou's Cracking Index Map produced with open-source pycalphad + COST507.tdb Solidification with no diffusion (Scheil).

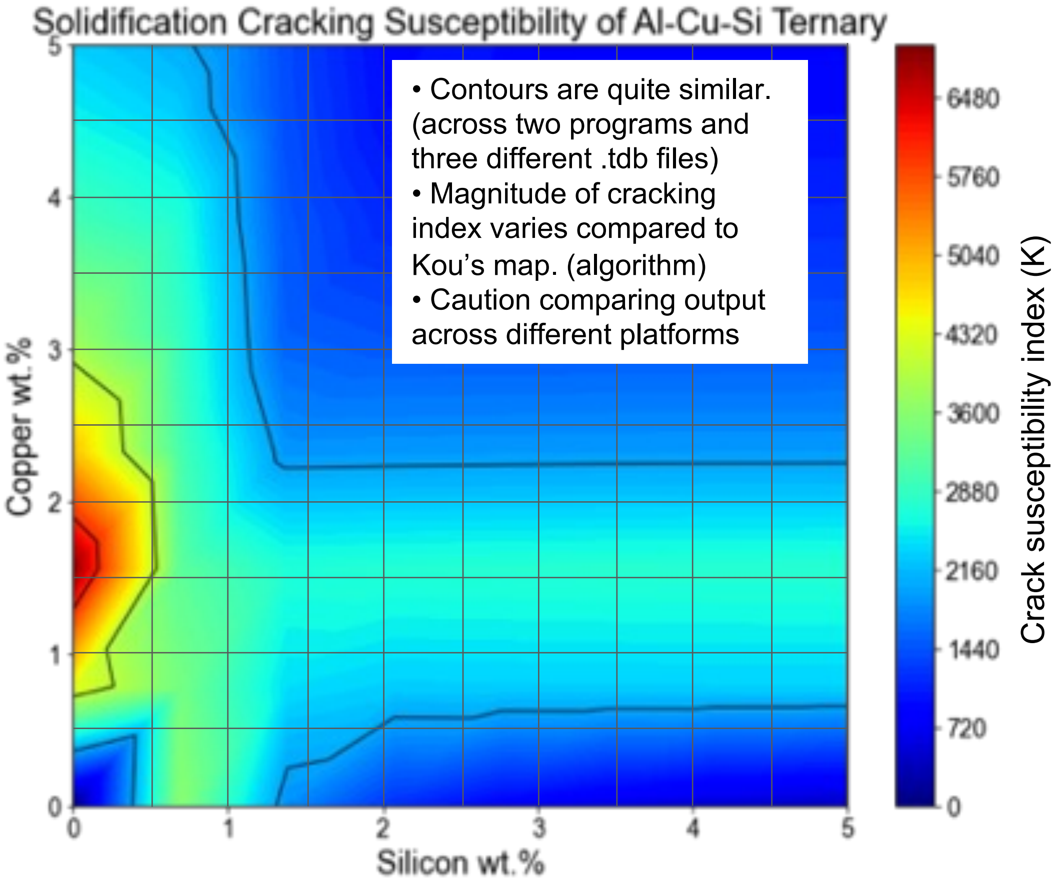

- Contours are quite similar. (across two programs and three different .tdb files)
- Magnitude of cracking index varies compared to Kou's map. (algorithm)
- Caution comparing output across different platforms

Two open-source TDB were tested producing similar map results:
[10] Ansara et al. (1998) COST 507.
[11] Hallstedt et al. *Calphad* 53 (2016): 25-38.

1. Algorithm Verification with Refractory Alloy Varestraint Data

- Lessman and Gold [12] published refractory metal Varestraint testing of seven refractory alloys subject to GTA welding in inert vacuum.

Refractory Alloy Compositions:

Alloy	Nominal Composition	Ta	Nb	W	Hf	Mo	Re	V	Zr	C ppm	O ppm	N ppm	C ppm	O ppm	N ppm
T-111	Ta-8W-2Hf	balance	-	8.2	2.0	-	-	-	-	40	80	12	33	40	12
ASTAR-811C	Ta-8W-1Re-0.7Hf-0.025C	balance	-	8.1	0.9	-	1.4	-	-	300	70	10	210	5	5
FS-85	Nb-27Ta-10W-1Zr	28.1	balance	10.6	-	-	-	-	0.94	20	90	60	32	53	47
T-222	Ta-9.6W-2.4Hf-0.01C	balance	-	9.2	2.55	-	-	-	-	115	50	20	119	17	11
B-66	Nb-5Mo-5V-1Zr	-	balance	-	-	5.17	-	4.89	1	95	110	63	37	120	70
Ta-10W	Ta-10W	balance	-	9.9	-	-	-	-	-	50	40	20	5	10	10
SCb-291	Nb-10W-10Ta	9.83	balance	10.0	-	-	-	-	-	20	110	40	22	101	20

- Themocalc (TCHEA6.tdb) was used to calculate Scheil solidification paths of those seven alloys and subsequent CSI. Oxygen was ***not*** in the database.
- CSI shows good correlation to Ta- and Nb-based refractory alloy Varestraint test data.
- Refractory alloys with CSI < 30*10³ K are weldable in practice.
- Refractory alloys with CSI > 80*10³ K would likely crack at all augmented strains.

[12] Lessman and Gold. *Welding J.* (1971): 1s – 8s.

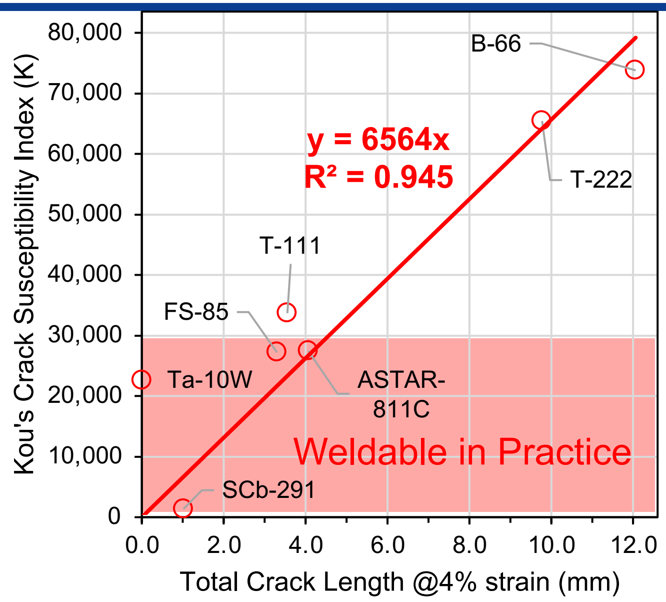

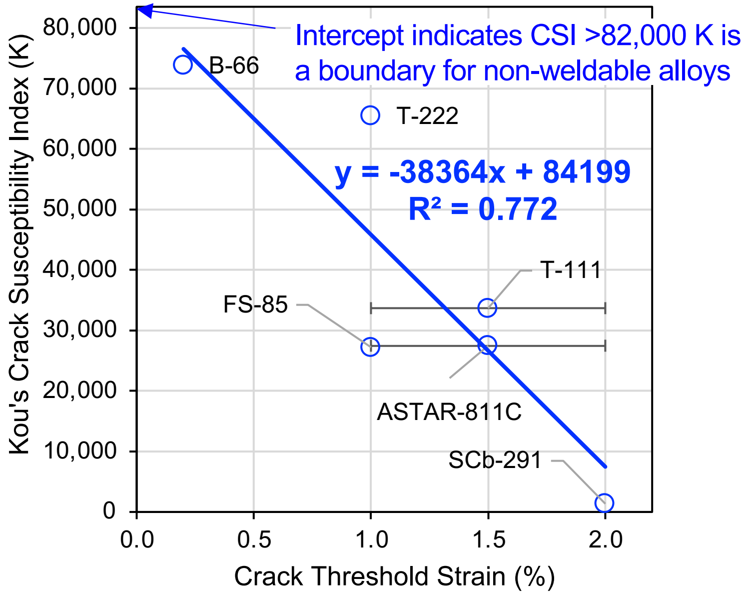

2. Crack Susceptibility Index in Binary Refractory Mixtures

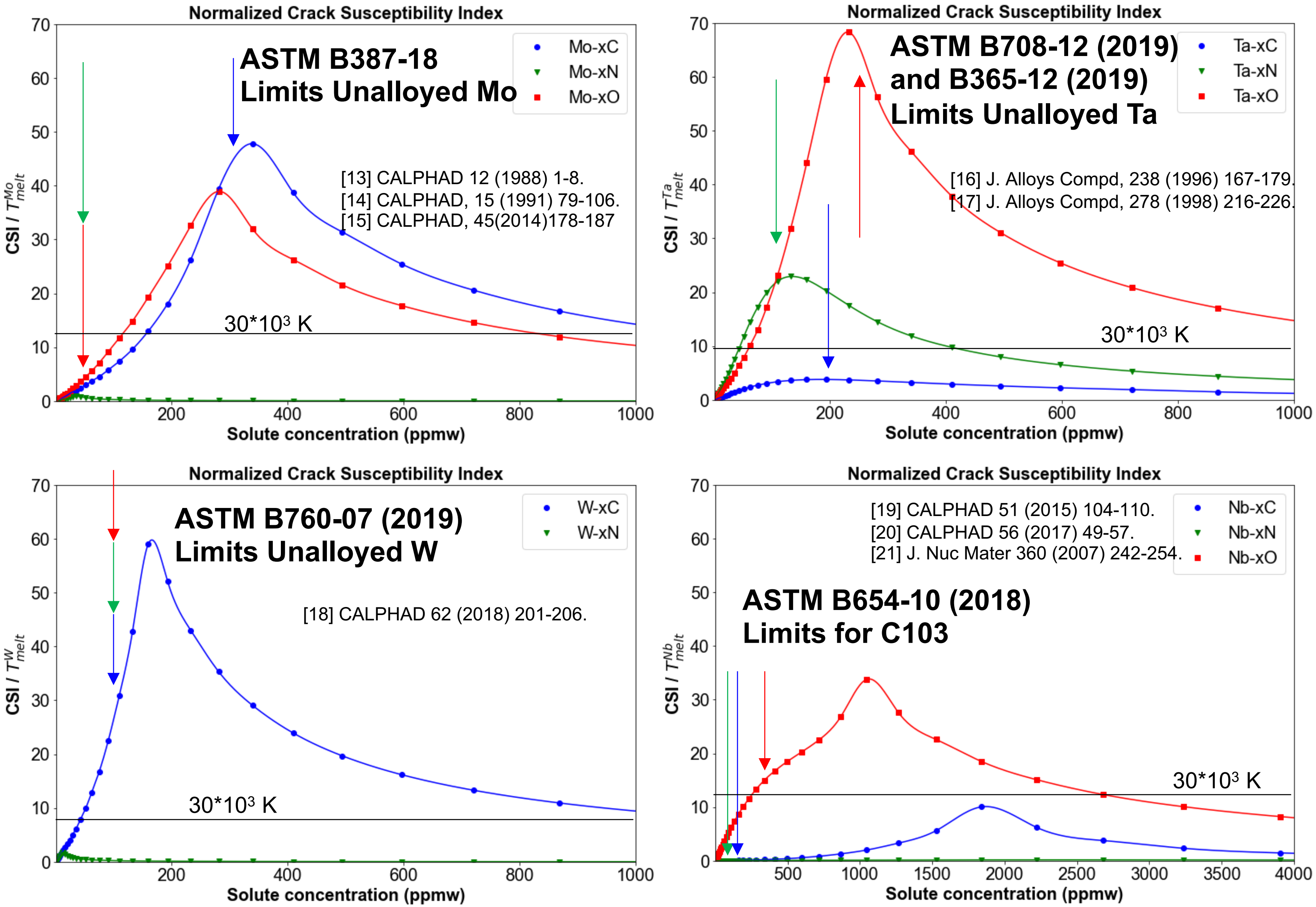

- Solidification cracking is strongly influenced by interstitial elements in practice
- CSI of C, N, O interstitial alloys
- CSI is normalized by T_{melt} for scaling
- Effect of interstitials as follows:

Effect of Carbon on CSI:
W > Mo > Ta > Nb

Effect of Nitrogen on CSI:
Ta > Mo > W > Nb

Effect of Oxygen on CSI (No W-O):
Ta > Mo > Nb

- Comparison to ASTM chemistry limits:

Mo: C Limit is near peak CSI
Ta: C, N, O limits are near peak CSI
W: C limit may be concern, O is unknown
Nb: O limit may be concern

- Additive powder recycling pickup of C and O especially will promote cracking.

3. Extending the Model: Chemistry-dependent Cracking

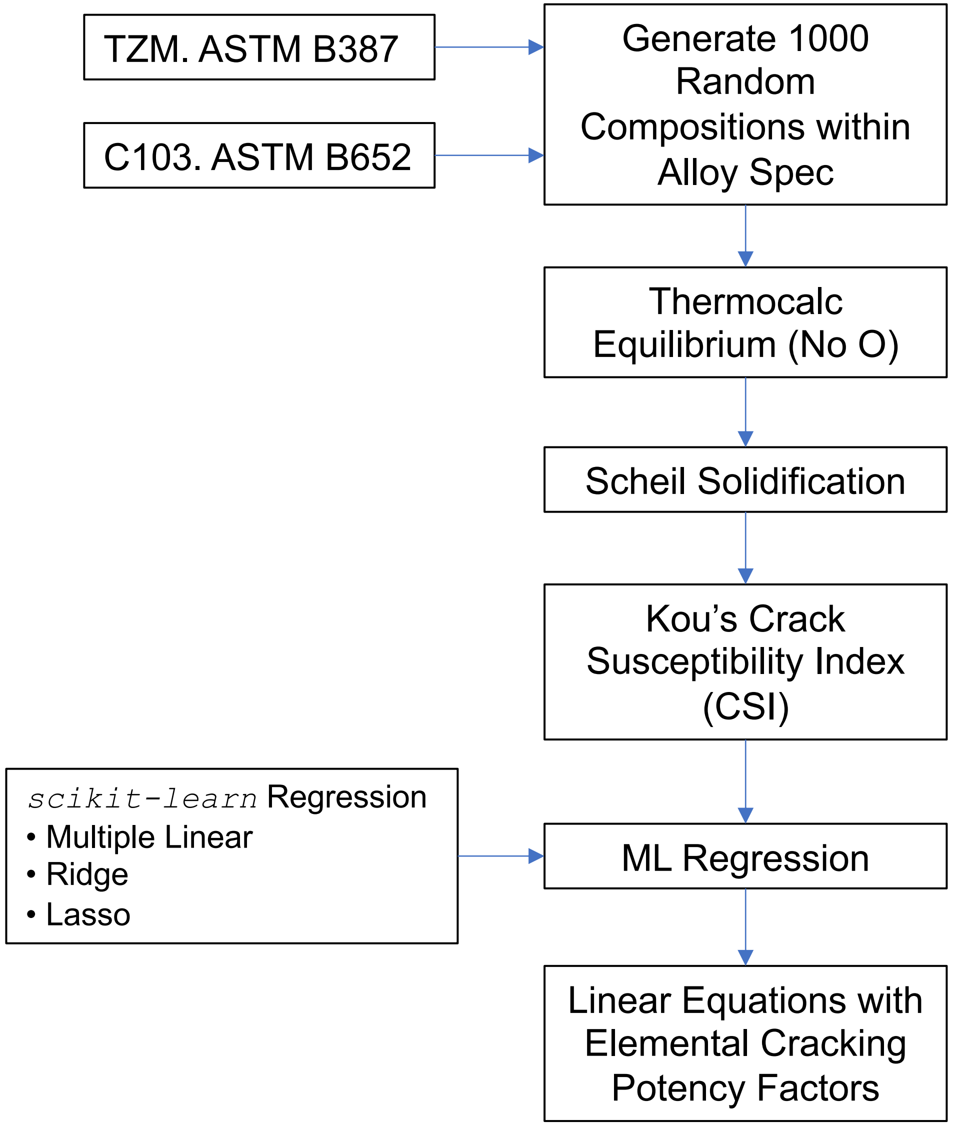

Many equations have been developed to relate solidification cracking to alloying elements through multiple linear regression [22].

[22] Matsuda (1990). Proc 1st US-Japan Symposium on Advances in Welding Metallurgy. 19-36.

Element	TZM Ingot - ASTM B387 (wt.%)
C	0.01 – 0.04
O*	0.003 max
N	0.002 max
Fe	0.01 max
Ti	0.4 – 0.55
Si	0.01 max
Ni	0.002 max
Zr	0.06 – 0.12
Mo	balance

*O in powder metallurgy alloy is 0.05 max

Element	C103 Ingot - ASTM B652 (wt.%)
C	0.015 max
O	0.025 max
N	0.010 max
H	0.0015 max
Hf	9 – 11
Ti	0.7 – 1.3
Zr	0.700 max
W	0.500 max
Ta	0.500 max
Nb	balance

Input and Results

TZM Distribution *N* = 1,000

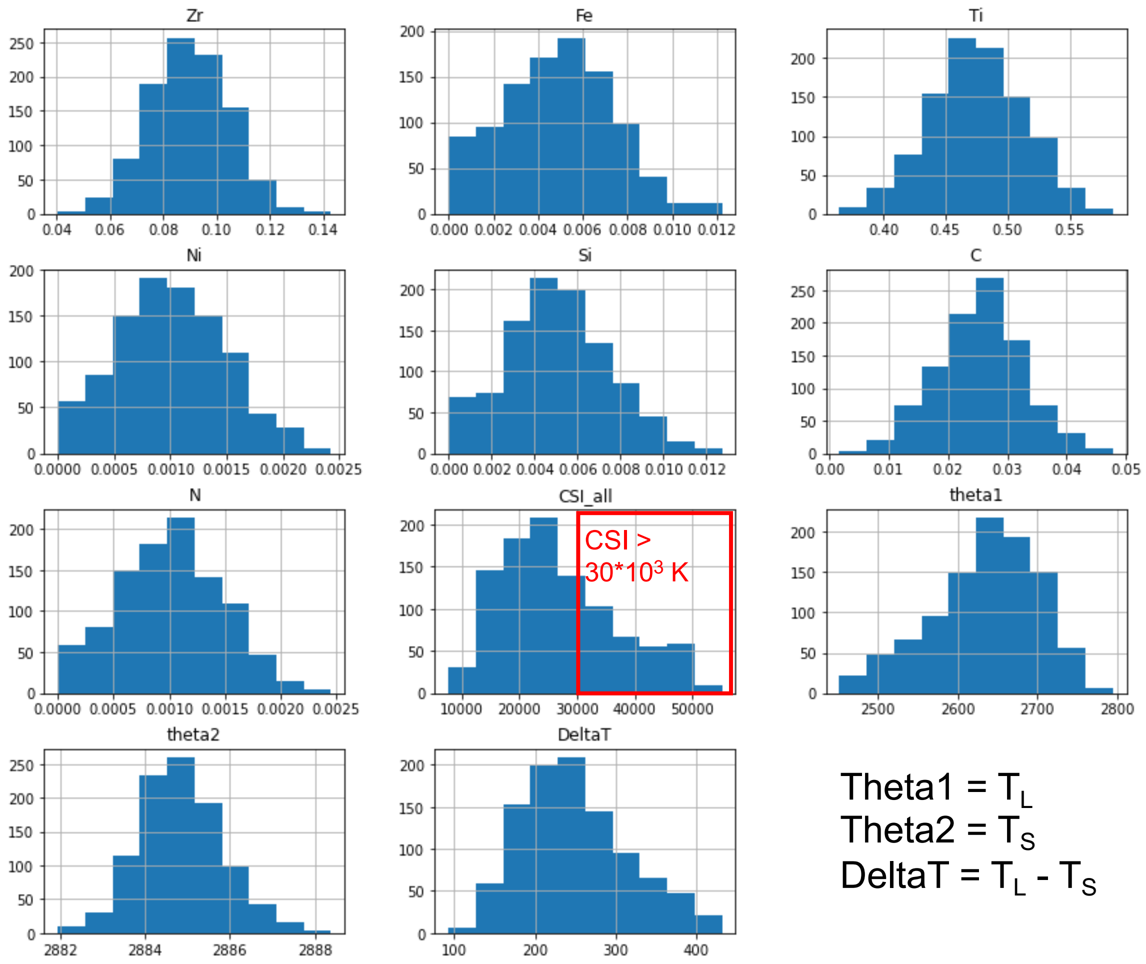

Theta1 = T_L
Theta2 = T_S
DeltaT = T_L - T_S

C103 Distribution *N* = 1,000

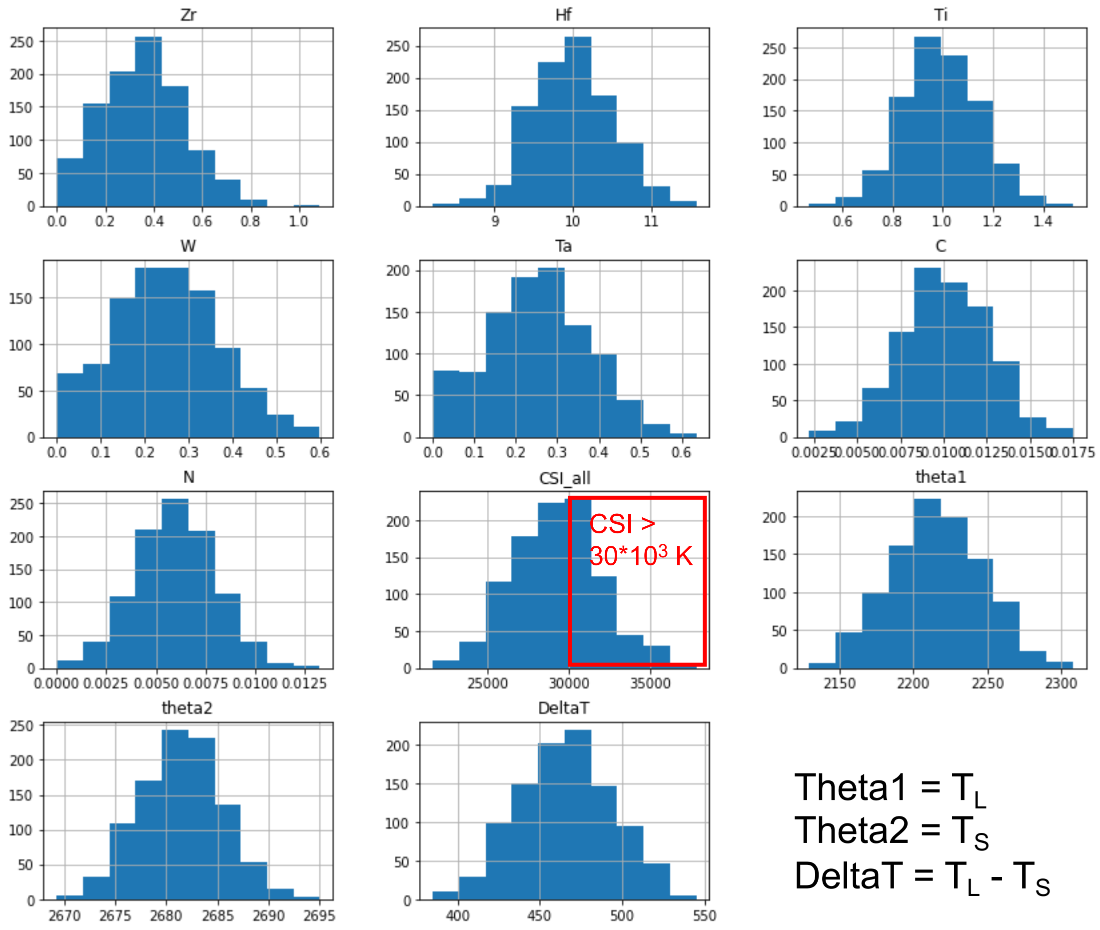

Theta1 = T_L
Theta2 = T_S
DeltaT = T_L - T_S

Negative values of composition are assumed zero. Data are normally distributed. A large portion of compositions produce a CSI > $30*10^3$ K.

Interaction Matrix to Determine Correlations

TZM

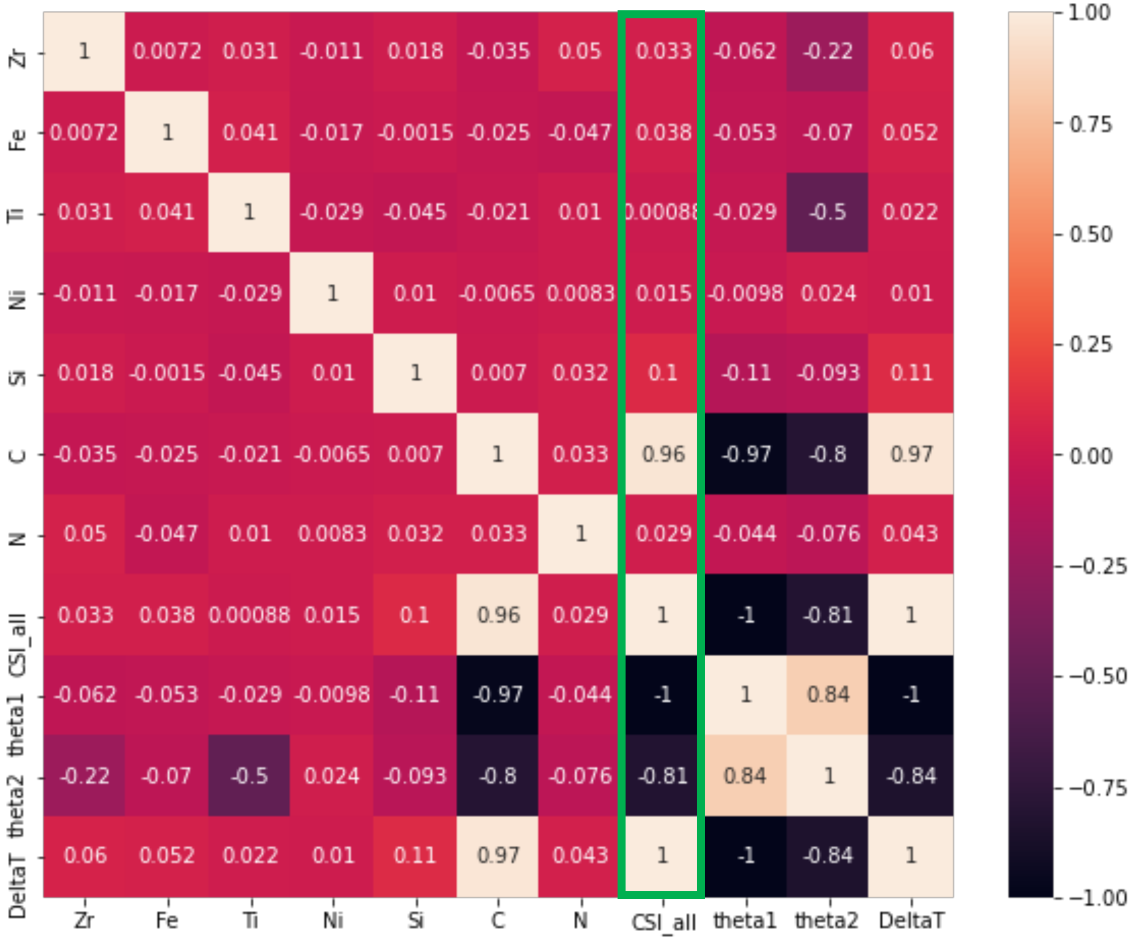

C103

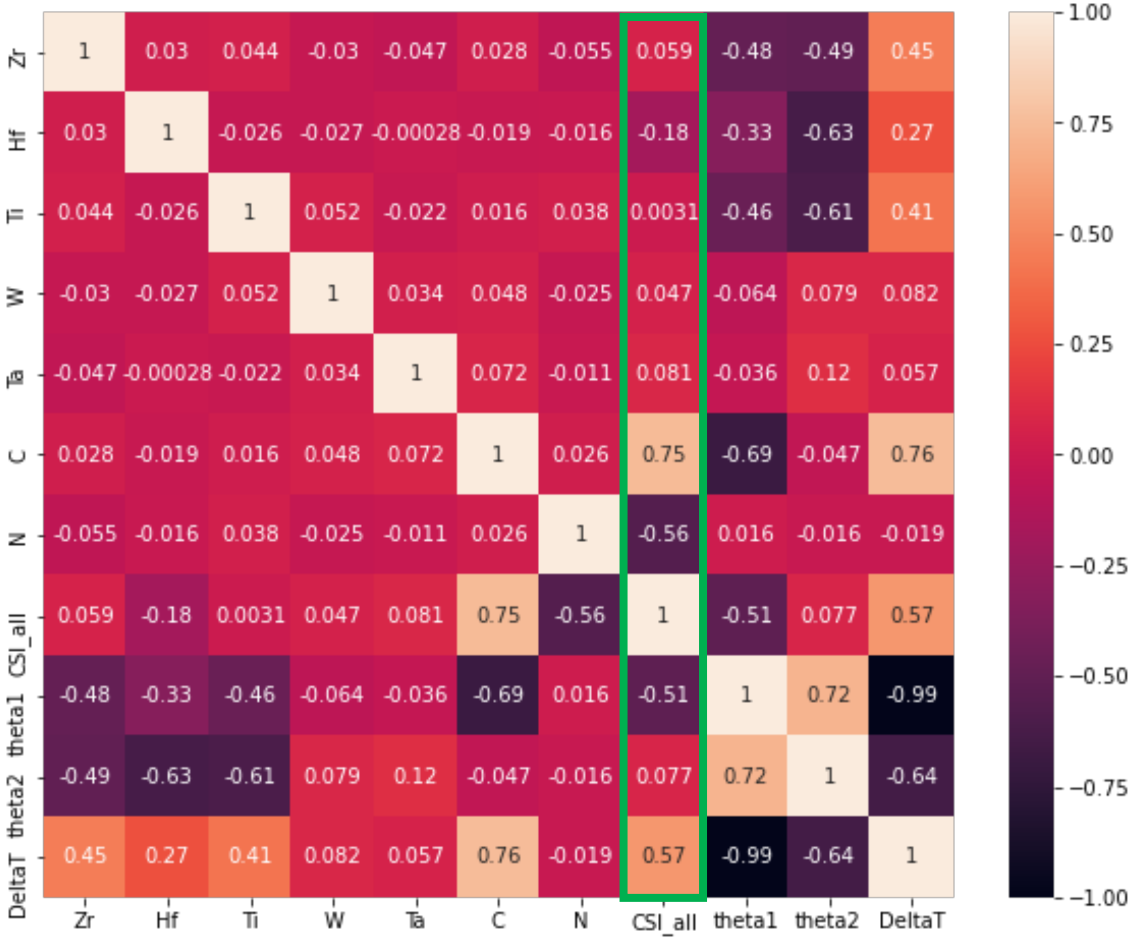

Multicollinearity (several independent variables are correlated) is not observed.

Regression Results and Best Fit Model

TZM

CSI = $\beta_0 + \beta_{Zr}X_{Zr} + \beta_{Fe}X_{Fe} + \beta_{Ti}X_{Ti} + \beta_{Ni}X_{Ni} + \beta_{Si}X_{Si} + \beta_C X_C + \beta_N X_N$
where X expressed in [wt.%]

Model	Linear	Ridge	Lasso
α	--	0.0001	0.0001
R^2	0.94774	0.94768	0.94774
β_0	-17066.3	-16805.1	-17065.8
β_{Zr}	43924.2	43753.9	43922.9
β_{Fe}	246464	242320	246450
β_{Ti}	5732.26	5657.58	5731.96
β_{Ni}	465135	325775	464705
β_{Si}	385805	379454	385787
β_C	1334869	1332153	1334866
β_N	-156242	-105938	-155788

C103

CSI = $\beta_0 + \beta_{Zr}X_{Zr} + \beta_{Hf}X_{Hf} + \beta_{Ti}X_{Ti} + \beta_W X_W + \beta_{Ta}X_{Ta} + \beta_C X_C + \beta_N X_N$
where X expressed in [wt.%]

Model	Linear	Ridge	Lasso
α	--	0.0001	0.0001
R^2	0.92197	0.92163	0.92197
β_0	34966.3	34977.1	34966.3
β_{Zr}	177.93	197.265	177.952
β_{Hf}	-960.084	-960.276	-960.083
β_{Ti}	160.762	153.071	160.747
β_W	-208.024	-186.839	-207.989
β_{Ta}	449.447	472.192	449.47
β_C	809597	796558	809580
β_N	-771158	-752294	-771133

All models produce excellent fits to data. As the alpha value → 0, for Ridge and Lasso the coefficients approached ordinary Least Squares Regression model. Linear multiple regression is selected for further discussion.

Discussion. Effect of Oxygen

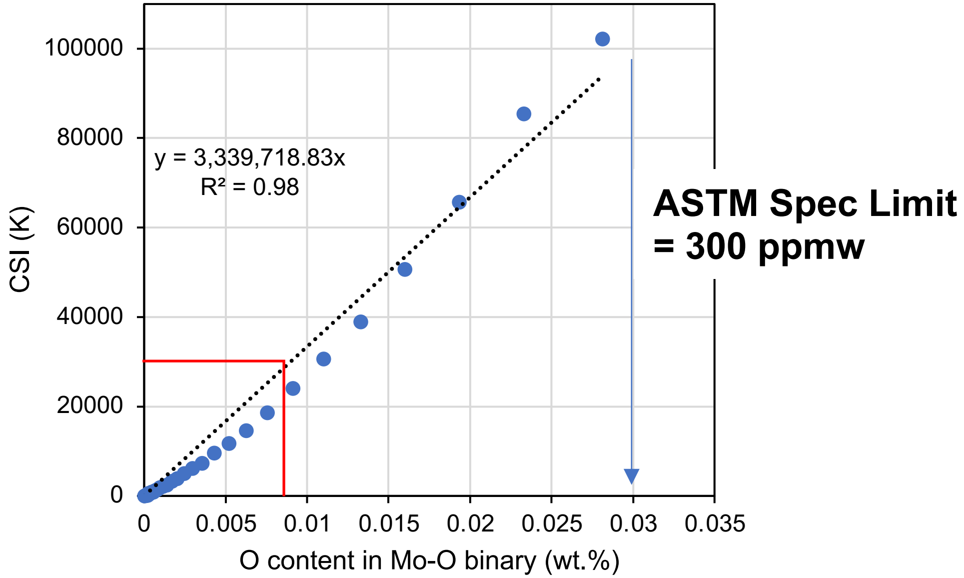

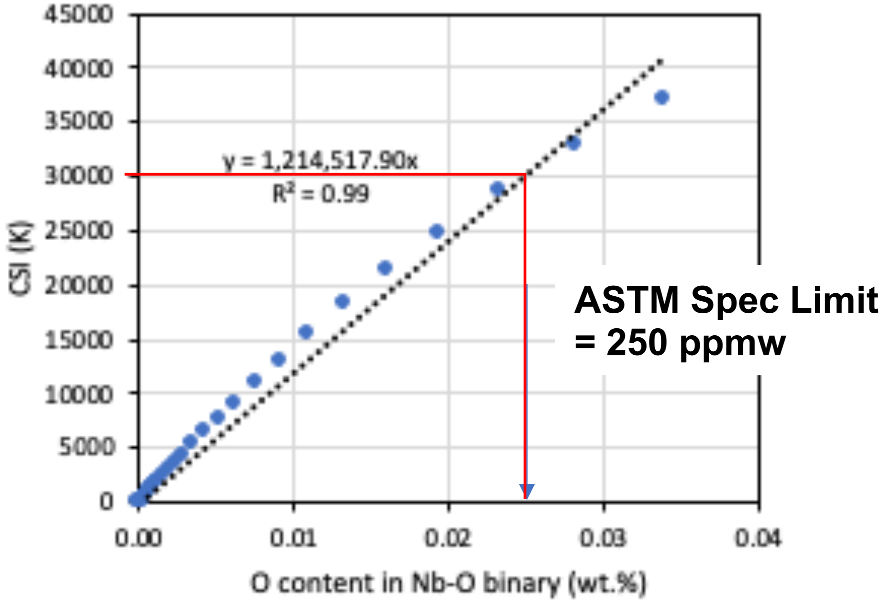

Oxygen was not considered in the complex alloys due to lack of available thermodynamic data for higher order mixtures. The Mo-O and Nb-O binary systems above show that oxygen drastically increases CSI.

We develop a weight factor based on linear interpolation above revealing a weight factor of 3.34×10^6 K/[O] and 1.21×10^6 K/[O], for Oxygen in TZM and C103, respectively.

Simplified Linear Models of Elemental Potency on Cracking

Steps:	TZM	C103
1. View Raw CSI coefficients. X_i in [wt. %]	CSI = -17,066 + 43,924 X_{Zr} + 246,464 X_{Fe} + 5,732 X_{Ti} + 465,135 X_{Ni} + 385,805 X_{Si} + 1,334,869 X_C - 156,242 X_N	CSI = 34,966 + 178 X_{Zr} - 960 X_{Hf} + 161 X_{Ti} - 208 X_W + 449 X_{Ta} + 809,597 X_C - 771,158 X_N
2. Modify with estimated oxygen term based on binary calculation. X_i in [wt. %]	CSI = -17,066 + 43,924 X_{Zr} + 246,464 X_{Fe} + 5,732 X_{Ti} + 465,135 X_{Ni} + 385,805 X_{Si} + 1,334,869 X_C + 3,339,718 X_O - 156,242 X_N	CSI = 34,966 + 178 X_{Zr} - 960 X_{Hf} + 161 X_{Ti} - 208 X_W + 449 X_{Ta} + 809,597 X_C + 1,214,518 X_O - 771,158 X_N
3. Normalize coefficients by max coefficient (Oxygen in both cases) revealing model with relative potency the alloying elements have on hot cracking susceptibility (HCS)	HCS = 0.013*Zr + 0.074*Fe + 0.002*Ti + 0.139*Ni + 0.116*Si + 0.4*C + O – 0.047*N	HCS = 0.667*C + O - 0.001*Hf – 0.635*N

- Oxygen and Carbon strongly promote solidification crack susceptibility.
- Nitrogen apparently decreases crack susceptibility especially in C103.
- Fe, Ni, Si promote crack susceptibility in TZM, as do Zr and Ti to lesser extent.

Summary

1. A numerical approach was developed to calculate Kou's Solidification Crack Susceptibility Index (CSI) using open-source Python code with both an open-source and a commercial CALPHAD equilibrium solver.
   - The method was verified against previous calculations and aluminum alloy solidification cracking data.
2. The numerical approach was applied to refractory metals, which are inherently difficult to study from a weldability testing standpoint since welding is often done in vacuum.
   - Calculated CSI showed strong empirical correlation to vacuum Varestraint testing of Ta- and Nb-alloys.
   - Correlations indicate that refractory alloys with CSI < 30×10^3 K are weldable in practice.
3. Calculation of CSI for refractory-interstitial (O,C,N) binary systems revealed ASTM chemistry specs are not ideal for optimal weldability and AM printability.
4. This work revealed the effect of compositional variations on a series of refractory metals and showed the framework defined here will be useful in:
   - The development of new alloys that have improved weldability and AM printability
   - Placing compositional limits on existing alloys
   - Consideration of manufacturing process controls such as powder reuse during 3D printing